Applied and Environmental Microbiology, May 2011, p. 2877–2881 Vol. 77, No. 9
0099-2240/11/$12.00 doi:10.1128/AEM.02867-10

Nanometer-Scale Visualization and Structural Analysis of the Inorganic/Organic Hybrid Structure of *Gallionella ferruginea* Twisted Stalks▽†

Tomoko Suzuki, Hideki Hashimoto, Nobuyuki Matsumoto, Mitsuaki Furutani, Hitoshi Kunoh, and Jun Takada*

Department of Material Chemistry, Graduate School of Natural Science and Technology, Okayama University, Okayama 700-8530, Japan

Received 8 December 2010/Accepted 24 February 2011

The so-called Fe/Mn-oxidizing bacteria have long been recognized for their potential to form extracellular iron hydroxide or manganese oxide structures in aquatic environments. Bacterial species belonging to the genus *Gallionella*, one type of such bacteria, oxidize iron and produce uniquely twisted extracellular stalks consisting of iron oxide-encrusted inorganic/organic fibers. This paper describes the ultrastructure of *Gallionella* cells and stalks and the visualized structural and spatial localization of constitutive elements within the stalks. Electron microscopy with energy-dispersive X-ray microanalysis showed the export site of the stalk fibers from the cell and the uniform distribution of iron, silicon, and phosphorous in the stalks. Electron energy-loss spectroscopy revealed that the stalk fibers had a central carbon core of bacterial exopolymers and that aquatic iron interacted with oxygen at the surface of the carbon core, resulting in deposition of iron oxides at the surface. This new knowledge of the structural and spatial associations of iron with oxygen and carbon provides deeper insights into the unique inorganic/organic hybrid structure of the stalks.

Some microorganisms convert metal ions to their oxidized forms by enzymatic removal of electrons, causing physicochemical reactions associated with the resulting change of the local pH (19). The so-called Fe/Mn-oxidizing bacteria have long been recognized for their potential to form extracellular iron hydroxide or manganese oxide structures in aquatic environments (5, 8, 12, 15, 16, 17). Bacteria belonging to the genus *Gallionella* are ubiquitous inhabitants of ocherous deposits that form in bodies of freshwater (5). They form a uniquely twisted extracellular iron oxide-encrusted bundle of fibers (commonly called a twisted stalk) (5). It is presently thought that the extracellular polysaccharides from the cell, which are the major organic components of the stalk, are closely linked with its mineralization by Fe, Si, and P (2, 4, 5, 7) and other minor elements (5). However, the structural origin and the presence of the stalk polysaccharides and the spatial association of elements within their structure remain unsolved in spite of a number of ultrastructural studies (2, 7, 11, 14, 18).

Iron-oxidizing bacteria such as *Gallionella*, *Leptothrix*, *Mariprofundus*, and *Rhodobacter* (3, 5, 8, 12, 15, 16, 17), with the ability to form extracellular iron oxides, have evoked great interest in biological and geochemical fields of research. The potential for future industrial use of these biologically derived iron oxides clearly indicates the need for detailed systematic study of the interactions of the biological organics with the aquatic metals and minerals in the stalks. The aim of this study is to examine the ultrastructure of *Gallionella* cells and stalks and to define the structural and spatial localization of constitutive elements within the stalks. Our analyses included the use of scanning electron microscopy (SEM)/transmission electron microscopy (TEM) with energy-dispersive X-ray (EDX) spectroscopy, high-angle annular dark-field scanning transmission electron microscopy (HAADF-STEM), and STEM electron energy-loss spectroscopy (STEM-EELS).

MATERIALS AND METHODS

Sampling sites and methods. Ocherous flocs associated with microbial mats attached to the wall of the groundwater-receiving tank were collected from a freshwater purification pilot plant at the farm of Okayama University (see Fig. S1 and S2 and Table S1 in the supplemental material). Although typical twisted stalks produced by *Gallionella ferruginea* were confirmed by light microscopy as the predominant deposits in the flocs, it was unavoidable that we would be looking at a mixed population because we were sampling natural products.

Light and electron microscopy. The collected samples were washed repeatedly with sterilized ultrapure water. The specimens were observed using a differential interference contrast microscope to confirm the prevalent presence of *G. ferruginea* stalks. For TEM, the precipitate was collected by centrifugation and fixed with a mixture of 2.5% glutaraldehyde, 1% OsO_4, and 4.5% sucrose in 100 or 60 mM cacodylate or phosphate buffer (pH 7.4) on ice for 2 h, followed by embedding in 2% agar. Small pieces of the washed agar block were dehydrated in a graded series of ethanol and again embedded in resin mixture. Ultrathin sections were stained with uranyl acetate and lead solution and then observed by TEM. For SEM, the suspension of the washed specimens was dropped onto an aluminum stub, vacuum dried, and Pt coated.

Structural and elemental analysis. A vacuum-dried uncoated specimen on a stub was subjected to analysis of element distribution in secondary electron images using an SEM/EDX detector.

The uranyl acetate-lead-stained ultrathin sections on copper grids were covered with a Formvar film and then coated with carbon. The sections were subjected to HAADF-STEM imaging and EDX elemental mapping by using a JEOL JEM-2100F TEM equipped with CEOS C_s corrector (for spherical correction) and an EDX detector (JED-2300T; JEOL), respectively.

For examination of the stalk suspension, a sample of the suspension was

* Corresponding author. Mailing address: Department of Material Chemistry, Graduate School of Natural Science and Technology, Okayama University, 3-1-1 Tsushima-naka, Kita-ku, Okayama 700-8530, Japan. Phone: 81 86 251 8106. Fax: 81 86 251 8087. E-mail: jtakada@cc.okayama-u.ac.jp.

† Supplemental material for this article may be found at http://aem.asm.org/.

▽ Published ahead of print on 4 March 2011.

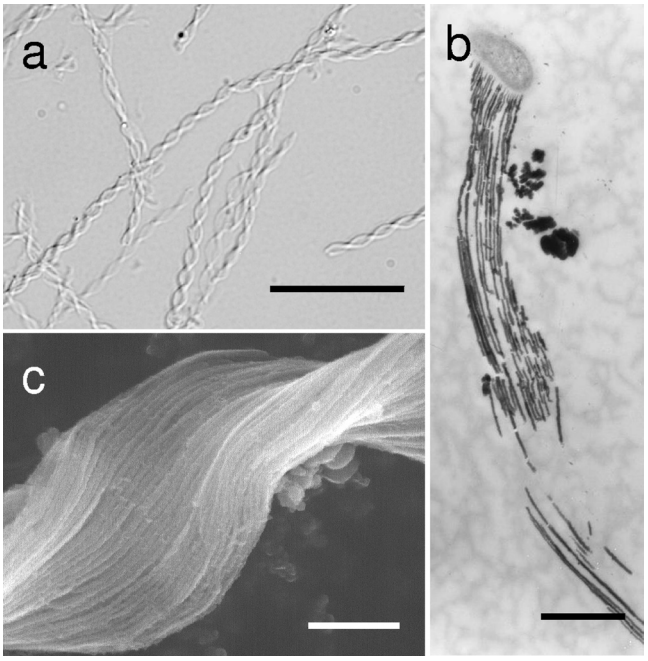

FIG. 1. Micrographs of *G. ferruginea* twisted stalks. (a) Light micrograph of typical twisted stalks of ocherous flocs collected from the groundwater-receiving tank (see Fig. S1 and S2 in the supplemental material). Scale bar, 20 μm. (b) TEM image of long stalk fibers originating from the concave side of the bacterial cell. Scale bar, 1 μm. (c) SEM image of closely arrayed, parallel long fibers of the twisted stalk. Scale bar, 0.5 μm.

dropped onto a copper grid covered with a carbon-coated porous thin membrane (NEM, Japan) and then vacuum dried. The stalk suspension was then subjected to HAADF-STEM imaging, followed by STEM-EELS mapping to examine distribution of C, O, and Fe within the stalks. High-spatial-resolution STEM and EELS analyses were performed using aberration-corrected STEM (JEM-2100F with CEOS C_s corrector) operated at 200 kV with an electron beam of about 0.3 nm. The EELS spectra of C, O, and Fe were acquired using a Gatan imaging filter ranging from 180 to 1,024 eV with a dispersion of 0.4 eV and a collection angle of 21 mrad. EELS mapping was performed using the Digiscan function of the Gatan digital micrograph software. The energies of the C-K, O-K, and Fe-$L_{2,3}$ edges are 284, 532, and 708 eV, respectively. The maps of C-K, O-K, and Fe-$L_{2,3}$ edges were reconstructed from the accumulated spectra on all pixels following the standard protocol of EELS quantitative analysis, which included subtracting background values.

RESULTS AND DISCUSSION

Ocherous flocs collected from the sampling site exhibited an assembly of twisted (tightly to loosely) or stretched ribbon-like stalks of irregular shapes and sizes (length, <10 to >200 μm; width, 0.5 to 3 μm) (Fig. 1a). The stalk comprised numerous electron-dense, closely arrayed, parallel fibers (20 to 100 nm thick) attached to a kidney-shaped bacterial cell (Fig. 1b and c). The high electron density of the fibers suggests deposition of heavy metals. The fibers were readily detached from the apical cells, and, thus, the cell-free stalks were most frequently observed in the flocs (Fig. 1a). Morphology of the stalks and fragility of the cell-stalk connection are very similar to features of *Mariprofundus ferrooxydans*, a stalk-forming iron bacterium, which was isolated from Fe^{3+}-rich microbial mats in the ocean in Hawaii (3). SEM/EDX detected major peaks of Fe and O and minor peaks of Si, P, and Ca in the fibers (see Fig. S3 in the supplemental material). This suggested that iron oxides were the major inorganic constituent of the fibers and that other minor elements were somehow linked with the fiber matrices.

Cross-sectional analysis revealed that the respective fibers emerged from the wall region with a low electron density (Fig. 2a) along the concave side of the bacterial cells (Fig. 1b and c). The fibers were extremely thin at their export sites from the

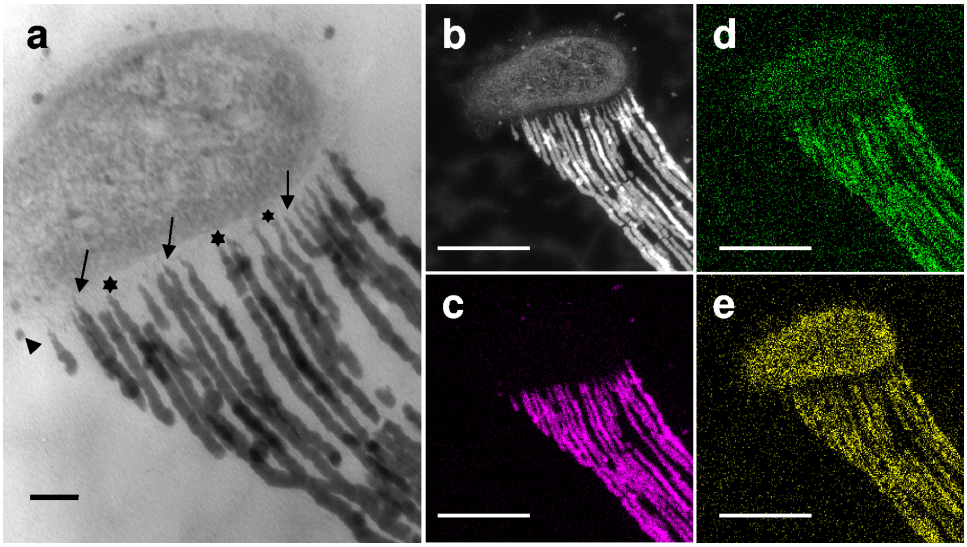

FIG. 2. TEM images and elemental maps showing the intimate association of the *G. ferruginea* cell and its stalk. (a) TEM image showing the connecting site of the bacterial mother cell and the fibers. Fibers originate from the wall region (stars) of the cell. At the export sites (arrows), fibers are extremely thin but become thicker within about 500 nm of the cell wall. (b) HAADF-STEM image of the cell with stretched stalk fibers from panel a. Note the uneven electron density of the fibers. Also shown are elemental maps of Fe (c), Si (d), and P (e) in the same image site with the same magnification as used for panel b. Note the following: (i) intense signals of Fe are detected in the fibers, but only traces are detected in the cell; (ii) a larger number of Si signals are detected in the fibers than in the cell; (iii) P is distributed almost evenly in the cell and fibers; and (iv) a noticeable number of Si and P signals occur in the background outside the cell and stalks. Scale bars, 0.1 μm (a) and 500 nm (b to e).

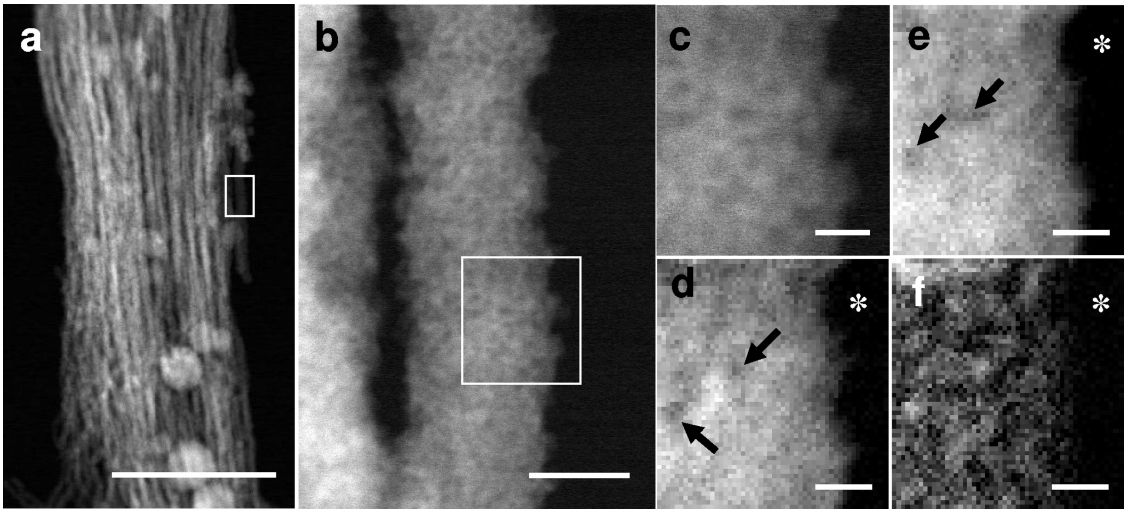

FIG. 3. HAADF-STEM images of the stalk fibers and STEM-EELS maps of Fe, O, and C in a single fiber. (a) HAADF-STEM image of a stalk comprised of fibers arrayed in parallel. Scale bar, 500 nm. (b) Enlarged HAADF-STEM image of a single fiber from the boxed area shown in panel a. Scale bar, 20 nm. (c) Enlarged HAADF-STEM image of the boxed area shown in panel b on which EELS mapping was performed. Shown are EELS spectrum images of Fe-$L_{2,3}$ (d), O-K (e), and C-K (f) edges. Fe and O are distributed relatively evenly, with some darker spots caused by the lower density of both elements but not by the absence of both elements (arrows) (d and e). C is distributed throughout, but intense signals of C are concentrated in places in the fiber core regions although not at the marginal edge (f). Asterisks in panels d to f indicate background areas without specimens. The precise localization of the target element can be defined by comparing the site density with the background darkness. Scale bar, 5 nm (c to f).

cell (Fig. 2a) but became thicker at a distance of approximately 500 nm from the export sites and elongated with a relatively consistent thickness thereafter, similarly to the stalk fibers of *M. ferrooxydans* (3). The clearly linear structure of the fibers (Fig. 1) suggests that the extracellular polymeric material comprising the fiber had a viscosity sufficiently high for protection from diffusion into the surrounding solution. Although Fig. 2a does not show the presence of pores in the *Gallionella* wall zone, this finding led us to hypothesize that the polymeric material could be excreted from the fine pores present in the bacterial cell wall in a manner similar to the excretion of cellulose fibers from *Acetobacter xylinus* cells (1, 9, 21).

Theoretically, the contrast in HAADF-STEM images depends on the square value of the atomic number (20). The fibers derived from a *Gallionella* cell, and not the cell itself, showed high contrast (Fig. 2b), suggesting that the fibers but not the cell contained considerable amounts of heavy metals. In the STEM-EDX distribution map (Fig. 2c), the elongated fibers show strong Fe signals, but the bacterial cell shows only traces. Lutters and Hanert (11) found that an intracytoplasmic membrane system invaginated from the concave side of the *Gallionella* cell and concluded that this system was involved in Fe^{2+} oxidation and Fe^{3+} excretion. Kucera and Wolfe (10) noted that *Gallionella* cells possessed the unusual ability to secrete twisted, Fe^{3+}-encrusted stalks. However, the current detection of trace Fe within cells in contrast to heavily concentrated Fe within fibers (Fig. 2b and c) suggests that intimate organic-metal/mineral interactions could occur outside the cells without intracellular deposition (2). This situation is similar to that of *M. ferrooxydans*, in which the Fe content is at trace levels in the cell but at relatively high levels in the stalk (3). Chan et al. (3) concluded that most of the Fe^{3+} from metabolic Fe oxidation (and abiotic mineralization) was located on the stalk.

In contrast, Si and P, which are essential elements for all organisms, are distributed in both the fibers and the cell (Fig. 2d and e), consistent with the SEM/EDX results presented in Fig. S3 in the supplemental material. The detection of Si and P signals in the background (outside the cell/stalk) likely reflects their ubiquitous presence in the sampled groundwater, from which they were not eliminated during specimen preparation. Note that Fig. 2d may include less precise information concerning Si distribution because overlapping of the proximal peaks of Si-Kα and Pb-M in the EDX spectrum cannot be avoided when Pb-stained sections are analyzed. Nevertheless, the presence of Si is undoubtedly supported by the SEM/EDX data obtained from uncoated dried specimens (see Fig. S3). Heterogeneous electron density (Fig. 2a and b) and uneven distribution (heavy to sparse) of each element in the fibers (Fig. 2c to e) may result from the irregular distribution of metals or minerals and/or from the uneven thickness of sectioned fibers at the analyzed plane because of the twisted form of the stalks. Si, but not P, was detected almost always in the *Gallionella* stalks (5, 14), whereas neither element was detected in the stalks of *M. ferrooxydans* (3). The constitutional difference of these ubiquitous elements in the stalks of both organisms, regardless of their structural similarity, could be attributable to preferential and selective affinity of the elements for the stalk, which may provide a clue to understanding the mechanism of stalk formation in both organisms.

In EELS mapping (Fig. 3d to f), fine, bright signal spots represent the sites of energy loss of the incident electron beam by the elements present. Because the energy loss for the respective elements occurs at specific electron voltages, the pre-

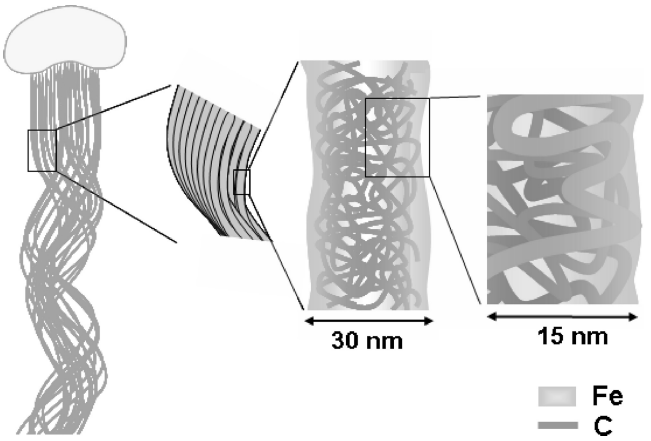

FIG. 4. Schematic of the putative carbon fibril network comprising a single fiber (approximately 30-nm width) of the stalk. Fibrils of a few nanometers were intermingled and folded at the fiber core region but not at the extreme margin. These C fibrils were excreted from the export pores located in the wall region of the bacterial cell. Oxidized iron could interact with C in the entire fiber.

cise nanometer-level localization of the specific element is defined by comparing the site density with the background darkness produced by the lack of the target element (Fig. 3d to f). Thus, the observation of some darker regions (Fig. 3d and e) indicates a lower density but not the absence of the target element. In the HAADF-STEM images (Fig. 3a and b), the parallel fibers measure 20 to 70 nm thick. For EELS analysis, a single fiber was selected from the framed STEM image (Fig. 3a and b). In an enlargement of the same image (Fig. 3b and c), some fine, darker spots of varied sizes were observed in the rather smooth, bright signal region. The heterogeneous brightness observed likely reflects a structural unevenness of the fiber matrix. In the Fe distribution map shown in Fig. 3d, darker spots with low electron density are apparent in some areas, indicating heterogeneous distribution of Fe over the entire fiber matrix. Oxygen in the fiber is distributed in a manner similar to Fe, but more evenly and with fewer low-density spots (Fig. 3e). In contrast, C distribution (Fig. 3f) is characterized by numerous signals, with a high concentration in some areas. Interestingly, the intense C signals are not detected at the marginal region, as is evident in comparisons of the images of Fig. 3c to f obtained from the same framed area at the same magnification, suggesting that C is localized in the core but to a lesser degree, or not at all, at the margin of the fiber. The concentrated distribution of C (Fig. 3f) led us to hypothesize that the fiber could consist of structural units that might form an intermingled or folded fibril C network of bacterial polysaccharides (Fig. 4). Moreover, the signal of regions of concentrated C could correspond to the crossing point of unit fibrils (Fig. 3f). According to current understanding, chemoautotrophic *Gallionella* uses Fe^{2+} as an energy source by oxidizing it to Fe^{3+} in the bacterial cells, most likely in the cell envelope, including the plasma membrane (2, 4, 6). However, the nearly identical localization patterns of Fe and O, even at the fiber margin (Fig. 3d and e), suggests that Fe oxidation might occur in the entire fiber, leading to the formation of iron oxides even at the fiber surface, and that the residual O might interact with the other elements including C, Si, and P. These hypotheses led us to assume that such oxidation processes might occur independently of the bacterial cells. Chan et al. (2) demonstrated colocalization of Fe and C on *Gallionella* stalks by scanning transmission X-ray microscopy and suggested that iron oxyhydroxide mineralization of the polysaccharide strands possibly explains the natural formation of mineralized structures. Our EELS mapping (Fig. 3) showing colocalization of Fe and O, rather than C, on a single fiber suggests that Fe could exist as iron oxide and/or oxyhydroxide in the fibers. Chan et al. (2) demonstrated that *Gallionella* polysaccharides spatially correlated with iron oxyhydroxide distribution patterns as determined by X-ray fluorescence microscopy, suggesting that organic fibrils could collect iron oxyhydroxide and control its recrystallization in the stalks. Likewise, Hallberg and Ferris (7) revealed minute flaky iron precipitates in the fibers by SEM and showed that the Fe/O atomic ratio is nearly 0.67 in individual crystallites, suggesting stoichiometric formulation of Fe_2O_3. Their conclusion (7) is not inconsistent with our Fe/O distribution pattern in Fig. 3d and e. They believed that with time the fibers became covered with iron oxyhydroxide because of inorganic, rather than organic, chemical processes within the stalk. These Fe ion conversion processes in the fibers are consistent with the report of Rentz et al. (13) that in *Gallionella* stalks and *Leptothrix* sheaths the abiotic oxidation included the chemical oxidation of aqueous Fe^{2+}, as well as the surface-mediated Fe^{2+} oxidation on abiogenic iron oxides. Chan et al. (3) presented a model of stalk formation and the mineralization process of *M. ferrooxydans* based on their systematic microscopical and spectroscopical work. In the model, they illustrated that as stalks aged, Fe oxyhydroxide minerals (for example, lepidocrocite) nucleated on the surfaces of fibrils and grew into larger crystals, whereas the minerals within the fibrils remained small, and that abiotic Fe oxidation was typical of Fe-oxidizing bacteria. Although their model serves as an invaluable reference for understanding the stalk formation of *Gallionella*, we certainly need to collect more basic data concerning the biotic versus abiotic oxidation of Fe catalysis and the spatial and structural linkages of inorganic and organic constituents in the fibers before considering a similar model for *Gallionella* stalks.

Si and P represent major inorganic components of fibers although they are present in lesser amounts than Fe (Fig. 2d and e), thus resembling their distributions in the *Leptothrix* sp. sheath (8, 15). However, further elucidation of the interactions of both elements with the fibers is certainly required, and it will provide significant insights relevant for the industrial use of the stalks as a novel functional material.

EELS technology provides a powerful analytical tool for understanding the nanometer-scale spatial relationships of constitutive elements in the stalks. Since the *in vitro* synthesis of *Gallionella* stalks has not been possible, our understanding of their structural and compositional associations will rely on future developments in three-dimensional tomographic construction of EELS maps.

ACKNOWLEDGMENTS

This study was financially supported by a Special Grant for Education and Research (2008.4-2013.3) from the Ministry of Education, Culture, Sports, Science, and Technology, Japan.

We are indebted to Naoyuki Miyata, Department of Biological Environment, Akita Prefectural University, Akita, Japan, for his critical reviewing of the manuscript and valuable suggestions.

REFERENCES

1. **Brown, R. M., Jr., J. H. M. Willison, and C. L. Richardson.** 1976. Cellulose biosynthesis in *Acetobacter xylinum*: visualization of the site of synthesis and direct measurement of the *in vivo* process. Proc. Natl. Acad. Sci. U. S. A. **73:**4565–4569.
2. **Chan, C. S., S. C. Fakra, D. C. Edwards, D. Emerson, and J. F. Banfield.** 2009. Iron oxyhydroxide mineralization on microbial extracellular polysaccharides. Geochim. Cosmochim. Acta **73:**3807–3818.
3. **Chan, C. S., S. C. Fakra, D. Emerson, E. J. Fleming, and K. J. Edwards.** 25 November 2010, posting date. Lithotrophic iron-oxidizing bacteria produce organic stalks to control mineral growth: implication for biosignature formation. ISME J. doi:10.1038/ismej.2010.173.
4. **Chan, C. S., et al.** 2004. Microbial polysaccharides template assembly of nanocrystal fibers. Science **303:**1656–1658.
5. **Ghiorse, W. C.** 1984. Biology of iron- and manganese-depositing bacteria. Annu. Rev. Microbiol. **38:**515–550.
6. **Hallbeck, L., and K. Pedersen.** 1990. Culture parameters regulating stalk formation and growth rate of *Gallionella ferruginea*. J. Gen. Microbiol. **136:** 1675–1680.
7. **Hallberg, R., and F. G. Ferris.** 2004. Biomineralization by *Gallionella*. Geomicrobiol. J. **21:**325–330.
8. **Hashimoto, H., et al.** 2007. Characteristics of hollow microtubes consisting of amorphous iron oxide nanoparticles produced by iron oxidizing bacteria, *Leptothrix ochracea*. J. Magn. Magn. Mater. **310:**2405–2407.
9. **Hirai, A., M. Tsuji, and F. Horii.** 2002. TEM study of band-like cellulose assemblies produced by *Acetobacter xylinum* at 4 °C. Cellulose **9:**105–113.
10. **Kucera, S., and R. S. Wolfe.** 1957. A selective enrichment method for *Gallionella ferruginea*. J. Bacteriol. **74:**344–349.
11. **Lutters, S., and H. H. Hanert.** 1989. The ultrastructure of chemolithoautotrophic *Gallionella ferruginea* and *Thiobacillus ferrooxidans* as revealed by chemical fixation and freeze-etching. Arch. Microbiol. **151:**245–251.
12. **Miot, J., et al.** 2009. Extracellular iron biomineralization by photoautotrophic iron-oxidizing bacteria. Appl. Environ. Microbiol. **75:**5586–5591.
13. **Rentz, J. A., C. Kraiya, G. W. Luther III, and D. Emerson.** 2007. Control of ferrous iron oxidation within circumneutral microbial iron mats by cellular activity and autocatalysis. Environ. Sci. Technol. **41:**6084–6089.
14. **Ridgway, H. F., and B. H. Olson.** 1981. Scanning electron microscopic evidence for bacterial colonization of a drinking-water distribution system. Appl. Environ. Microbiol. **41:**274–287.
15. **Sakai, T., et al.** 2010. Chemical modification of biogenous iron oxide to create an excellent enzyme scaffold. Org. Biomol. Chem. **8:**336–338.
16. **Spring, S.** 2006. The genera *Leptothrix* and *Sphaerotilus*, p. 758–777. *In* M. Dworkin, S. Falkow, E. Rosenberg, K.-H. Schleifer, and E. Stackebrandt (ed.), The prokaryotes, 3rd ed., vol. 5. Springer Science, New York, NY.
17. **van Veen, W. L., E. G. Mulder, and M. H. Deinema.** 1978. The *Sphaerotilus-Leptothrix* group of bacteria. Microbiol. Rev. **42:**329–356.
18. **Vatter, A. E., and R. S. Wolfe.** 1956. Electron microscopy of *Gallionella ferruginea*. J. Bacteriol. **72:**248–252.
19. **Wang, J., G. Muyzer, P. L. E. Bodelier, and H. J. Laanbroek.** 2009. Diversity of iron oxidizers in wetland soils revealed by novel 16S rRNA primers targeting *Gallionella*-related bacteria. ISME J. **3:**715–725.
20. **Weyland, M.** 2002. Electron tomography of catalysts. Top. Catal. **21:**175–183.
21. **Zaar, K. J.** 1979. Visualization of pores (export sites) correlated with cellulose production in the envelope of the gram-negative bacterium *Acetobacter xylinum*. J. Cell Biol. **80:**773–777.